IEEE Access
Multidisciplinary ⋮ Rapid Review ⋮ Open Access Journal

Received December 17, 2020, accepted January 1, 2021, date of publication January 8, 2021, date of current version January 14, 2021.

Digital Object Identifier 10.1109/ACCESS.2021.3049913

Adaptive Robust Constraint Following Control for Omnidirectional Mobile Robot: An Indirect Approach

FANGFANG DONG[1], DONG JIN[1], XIAOMIN ZHAO[2], AND JIANG HAN[1]
[1]School of Mechanical Engineering, Hefei University of Technology, Hefei 230009, China
[2]School of Automotive and Transportation Engineering, Hefei University of Technology, Hefei 230009, China

Corresponding author: Xiaomin Zhao (xiao_min_zhao@163.com)

This work was supported in part by the National Natural Science Foundation of China under Grant 51905140, in part by the National Key Research and Development Program of China under Grant 2018YFB1308400, in part by the Natural Science Foundation of Anhui Province under Grant 1908085QF267, in part by the University Synergy Innovation Program of Anhui Province under Grant GXXT-2019-031, and in part by the Fundamental Research Funds for the Central Universities of China under Grant PA2020GDSK0090 and Grant JZ2020YYPY0107.

ABSTRACT The tracking performance of mobile robot is often affected by uncertainties from the deviation of initial conditions, external disturbances and varying loads, etc. An Udwadia-Kalaba based adaptive robust control is proposed for the trajectory tracking of an omnidirectional mobile robot in the presence of uncertainties. The proposed control includes nominal control part based on Udwadia-Kalaba theory and adaptive robust control part. The desired trajectory is considered as a virtual servo constraint applied to the robot system and converted into the second order standard form. So that the analytical form of constraint force could be obtained via Udwadia-Kalaba Fundamental Equation (UKFE). The system will precisely obey the given constraint (i.e., the desired trajectory) under the obtained constraint force in ideal cases. No auxiliary variables are required and it is effective whether the constraints are holonomic or nonholonomic. The designed adaptive law is in leakage type and the adaptive parameters are adjusted according to the performance of the system in order to compensate for the effect caused by uncertainty in the system. No extra information of uncertainty is needed except for the existence of uncertainty bound. Comparing with PID control, it can be found that the proposed control has better performance and can realize higher precision trajectory tracking control.

INDEX TERMS Udwadia-Kalaba theory, adaptive robust control, constraint following, uniformly bounded, uncertainty.

I. INTRODUCTION

Benefitting from its characteristics of moving in any direction, omnidirectional mobile robots have more advantages than traditional mobile platforms. Therefore, they have been widely used in the fields of industry, medicine, and aerospace in recent years. In the robot system, the tracking control of robot has always been a hotspot. An enormous number of approaches to realize the tracking control of robots have been reported in the past decades. For example, in Reference [1], the actual position of a mobile robot was evaluated by radio frequency identification technology, and the trajectory of robot was planned by sliding mode control. The dynamics of differential steering mobile robot was analyzed, and a fuzzy control method was proposed in Reference [2]. The joint simulation platform verified that the method could be used for the trajectory planning control. In Reference [3], Bang-bang Control was applied to achieve the trajectory generation and path planning of a three-wheeled omnidirectional mobile.

As for traditional methods of the trajectory tracking controls, the error of prescribed trajectory and feedback signal are utilized directly. From a quite different view, the prescribed trajectory is first treated as a virtual servo constraint and then is applied to the mobile robot system in this work. The controller is designed to provide the ideal constraint force which makes the system obey the system constraints (i.e., the desired trajectory). Such an indirect approach to use the given trajectory is so called the constraint-following control.

The associate editor coordinating the review of this manuscript and approving it for publication was Haibin Sun.

The design work is formulated to identify the constraint force under ideal or non-ideal constraints. The Udwadia-Kalaba Fundamental Equation (UKFE) is a powerful tool to achieve such purpose. The UKFE [4]–[6] was put forward in the 1990s and is a significant breakthrough in analytical mechanics. It gives the basic motion equations of multi-body systems under ideal or non-ideal constraints. By transforming the constraints into the second order standard form, the analytical solution of constraint force could be obtained no mater the constraint is holonomic or nonholonomic, ideal or nonideal. The UKFE is not only effective in control design, but also in dynamical modeling of mechanical systems. For example, in reference [7], the dynamic model of the three-wheel steering car was obtained by U-K theory, and then the trajectory tracking control of the vehicle was carried out by using UKFE. In reference [8], an adaptive controller was designed based on UKFE for constraint tracking of differential mobile robot.

In practical application, uncertainty arises due to the existence of varying loads, external interferences and mechanical errors, etc. Thus, the controller based on ideal condition can not achieve the expected performance. Many scholars began to bridge the gap between the ideal and the reality. In [9], a robust adaptive controller was designed, which was composed of disturbance observer and adaptive compensator. In the experiment, it can track and control the wheeled mobile robot with uncertainty. Reference [10] used linear extended state observers to evaluate the uncertainty of the differential robot. On this basis, an adaptive sliding mode control method was used to compensate the uncertainty to realize the trajectory tracking. In [11], an adaptive controller was designed for the trajectory tracking of an autonomous vehicle. After processing the expected motion parameter values of the vehicle, the controller used the updated values for the real-time control and the uniform ultimate boundedness was achieved. The adaptive neural network method was used to control different mechanical systems, and it was verified that the performance could be better under full state constraints in [12]. According to [13], a real-time navigation and trajectory tracking controller for nonholonomic mobile robot based on biological excitation was proposed by combining back-stepping technology with neural dynamics.In addition, fuzzy theory is also a popular method to deal with uncertainty, such as [14], [15]. The stability of the system was proved via Lyapunov minimax approach. A robust controller based on UKFE was proposed in [16]. And then, a performance index, incorporating fuzzy and deterministic performance, was designed to solve the optimal design of the proposed control. The effectiveness of the joint utilization of UKFE and various control methods, such as optimal control, fuzzy control, etc., was also verified in [17]–[21].

The contributions of this work are as follows. Firstly, being different from the traditional approaches which take the trajectory tracking error as the state variable, the proposed control is designed in an indirect way by abstracting the desired trajectory as a servo constraint. Secondly, the required constraint force is obtained by using UKEF so that the system will obey the constraint of given trajectory. This approach is indirect, simple and effective no matter the constraint is holonomic or nonholonomic. Thirdly, an adaptive robust control term is introduced to enhance the performance when uncertainty arises. No more information about uncertainty is required except for the existence of its uncertainty bound. The uniform boundedness and uniform ultimate boundedness are ensured when the proposed control is exerted. The remaining sections are organized as follows: In the second section, the dynamic model of three wheeled omnidirectional mobile robot is established. In the third section, an adaptive robust controller based on Udwadia-Kalaba theory is designed. The fourth section proves the stability of the controller via Lyapunov function, which satisfies uniform stability and uniform asymptotic stability. The fifth section verifies the effectiveness of this approach by numerical simulation.

II. DYNAMIC MODEL

Fig.1(a) and Fig.1(b) show a three wheeled omnidirectional mobile robot and its structure diagram respectively. The angle between the axes of adjacent omnidirectional wheels is 120° and the centers of the omnidirectional wheels are distributed on the same circle. The axis of the wheels points to the center of the robot. The three omnidirectional wheels are driven by DC motors. Thus, the robot not only can move along the tangent direction of the wheel surface, but also along the axis direction of the wheel. Through the combination of these two basic motion modes, the robot can move in any direction in the plane.

TABLE 1. Symbols and definitions of each parameter of the robot.

Parameter name	Physical meaning
A,B,C	Three omnidirectional wheels
θ	Robot attitude angle
Φ	The angle between the omnidirectional wheel and the equilateral triangle constructed by the robot
m	Total mass of robot
L	Distance from omnidirectional wheel to robot center point
I	Moment of inertia of the robot around the center
X	X-axis coordinates of robot center point in earth coordinate system
Y	Y-axis coordinates of robot center point in earth coordinate system
F_A, F_B, F_C	Each driving force of the three wheels
U_A, U_B, U_C	Each driving voltage of the three motors
V_A, V_B, V_C	The speed of the three wheels
V_x, V_y	Velocity components of each axis in robot coordinate system
ω	Angular velocity of robot rotation

Select $\chi = (X, Y, \theta)^T$ as the generalized coordinate to describe the shape and position of the robot. The robot coordinate system is $X_oO_oY_o$, the earth coordinate system is XOY, and the counterclockwise rotation is positive. The symbols and definitions of each parameter of the robot are shown in Table 1.

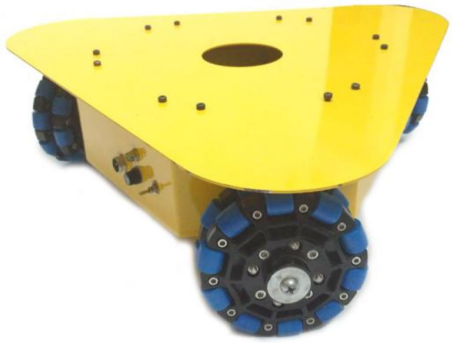

(a)

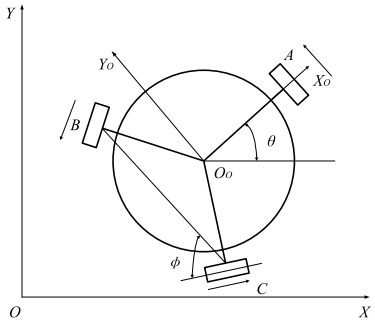

(b)

FIGURE 1. An omnidirectional wheeled mobile robot.

From the geometric characteristics of Fig.1(b), the relationship between the speed of the robot in the earth coordinate system and the speed in its own coordinate system is: $V_x = \dot{X}\cos\theta + \dot{Y}\sin\theta$, $V_y = -\dot{X}\sin\theta + \dot{Y}\cos\theta$, and the rotation angular velocity of the robot $\omega = \dot{\theta}$. These relationships could be expressed in matrix form:

$$\begin{bmatrix} V_x \\ V_y \\ \omega \end{bmatrix} = \begin{bmatrix} \cos\theta & \sin\theta & 0 \\ -\sin\theta & \cos\theta & 0 \\ 0 & 0 & 1 \end{bmatrix} \begin{bmatrix} \dot{X} \\ \dot{Y} \\ \dot{\theta} \end{bmatrix}. \tag{1}$$

In the robot coordinate system, we decompose the velocity component of each axis into the velocity direction of each wheel, and we can get the relationship between them:

$$\begin{bmatrix} V_A \\ V_B \\ V_C \end{bmatrix} = \begin{bmatrix} 0 & 1 & L \\ -\sin\phi & -\cos\phi & L \\ \sin\phi & -\cos\phi & L \end{bmatrix} \begin{bmatrix} V_x \\ V_y \\ \omega \end{bmatrix}. \tag{2}$$

According to (1) and (2), the relationship between the speed of each wheel and the generalized coordinates is:

$$\begin{bmatrix} V_A \\ V_B \\ V_C \end{bmatrix} = \begin{bmatrix} -\sin\theta & \cos\theta & L \\ \sin(\theta-\phi) & -\cos(\theta-\phi) & L \\ \sin(\theta+\phi) & -\cos(\theta+\phi) & L \end{bmatrix} \begin{bmatrix} \dot{X} \\ \dot{Y} \\ \dot{\theta} \end{bmatrix}. \tag{3}$$

The driving force of each wheel generated by the DC motor can be simplified as the following model [3]:

$$F = T_1 U - T_2 V, \tag{4}$$

where F is the driving force exerted on the omnidirectional wheel by the DC motor, V is the linear velocity of the corresponding wheel, U is the corresponding voltage applied to the motor, T_1 and T_2 are constants determined by the type of motor and the geometric model of the robot.

In the case of pure rolling between each wheel and the ground, the sum external force moment of mobile robot is generated by the three driving wheels:

$$I\ddot{\theta} = (F_A + F_B + F_C)L. \tag{5}$$

Unlike traditional wheeled robots, the speed direction of the omnidirectional mobile robot is arbitrary and not necessarily perpendicular to the axis of the driving wheel. It is difficult to find the relationship between the velocity and its generalized coordinates. Therefore, we give the relationship between the driving force and the acceleration in the earth coordinate system. According to the structural characteristics of the robot, the net force generated by the three wheels could be decomposed along the direction of the earth coordinate system. Then, we can get the relationship between the acceleration components (i.e., X and Y axes) and the generalized coordinates as follows:

$$\begin{cases} m\ddot{X} = [F_A\cos\theta - F_B\cos(\theta-\phi) - F_C\cos(\theta+\phi)] \\ m\ddot{Y} = [-F_A\sin\theta + F_B\sin(\theta-\phi) + F_C\sin(\theta+\phi)]. \end{cases} \tag{6}$$

According to (3), (4), (5) and (6), a general form (the second-order type) of mechanical system is obtained:

$$\begin{bmatrix} m & 0 & 0 \\ 0 & m & 0 \\ 0 & 0 & I \end{bmatrix} \begin{bmatrix} \ddot{X} \\ \ddot{Y} \\ \ddot{\theta} \end{bmatrix} + \frac{3T_2}{2} \begin{bmatrix} 1 & 0 & 0 \\ 0 & 1 & 0 \\ 0 & 0 & 2L^2 \end{bmatrix} \begin{bmatrix} \dot{X} \\ \dot{Y} \\ \dot{\theta} \end{bmatrix} = T_1 \begin{bmatrix} -\sin\theta & \sin(\theta-\phi) & \sin(\theta+\phi) \\ \cos\theta & -\cos(\theta-\phi) & -\cos(\theta+\phi) \\ L & L & L \end{bmatrix} \begin{bmatrix} U_A \\ U_B \\ U_C \end{bmatrix}. \tag{7}$$

III. CONTROLLER DESIGN

The uncertainty is an inevitable problem in mechanical system when designing the controller. Suppose a general mechanical system with uncertainty is expressed as follows:

$$M(\chi(t), \delta(t))\ddot{\chi}(t) + C(\dot{\chi}(t), \chi(t), \delta(t))\dot{\chi}(t) + G(\chi(t), \delta(t)) = \tau(t), \tag{8}$$

where $t \in \mathbf{R}$ is the time, $\chi(t) \in \mathbf{R}^n$ stands for the coordinate reflecting the shape and position of the system ($n = 3$ in this work), $\dot{\chi}(t)$ is the corresponding velocity, $\ddot{\chi}(t) \in \mathbf{R}^n$ is the corresponding acceleration, $\delta(t) \in \Sigma \subset \mathbf{R}^k$ is the parameter describing the uncertainty of the system, and Σ is the possible boundary set of $\delta(t)$. Furthermore, $\tau(t) \in \mathbf{R}^n$ is the control input of the system, $M(\chi, \delta)$ is the inertia matrix, $C(\dot{\chi}, \chi, \delta)\dot{\chi}$ is the Coriolis force or centrifugal force, $G(\chi, \delta)$ is the gravitational force. The dimensions of $M(\chi, \delta)$, $C(\dot{\chi}, \chi, \delta)$, $G(\chi, \delta)$ are determined by the specific occasions.

Assumption 1: For $\chi \in \mathbf{R}^n$ and $\delta \in \Sigma$, the matrix $M(\chi, \delta)$ is positive definite.

For the uncertain system, the matrices M, C and G are all consisted of two parts (the nominal part and the uncertain part) [22]:

$$M(\chi, \delta) = \bar{M}(\chi) + \tilde{M}(\chi, \delta),$$

$$C(\dot{\chi}, \chi, \delta) = \bar{C}(\dot{\chi}, \chi) + \tilde{C}(\dot{\chi}, \chi, \delta),$$
$$G(\chi, \delta) = \bar{G}(\chi) + \tilde{G}(\chi, \delta), \quad (9)$$

where $\bar{M}(\chi)$ is the nominal part (i.e., the known quantity), $\tilde{M}(\chi, \delta)$ is the uncertain part, and so is the matrix C and G. Now we define the following variables:

$$P(\chi) = \bar{M}^{-1}(\chi),$$
$$\tilde{P}(\chi, \delta) = M^{-1}(\chi, \delta) - \bar{M}^{-1}(\chi),$$
$$D(\chi, \delta) = \bar{M}^{-1}(\chi)M^{-1}(\chi, \delta) - I.$$

The trajectory that the mechanical system needs to satisfy is given as follows:

$$\sum_{i=1}^{n} E_{li}(\chi, t)\chi = d_l(\chi, t), \quad l = 1, \ldots, m(m \le n). \quad (10)$$

The above trajectory, i.e., Equation (10), can be treated as the system constraint. It can be further written as: $E(\chi, t)\chi = d(\chi, t)$, where $E = [E_{li}]_{m\times n}$, $d = [d_1, d_2, \ldots, d_m]^T$. Notice that this is a zero-order form constraint. Its corresponding first-order form is obtained after taking the derivative of the zero-order form with respect to time t:

$$\sum_{i=1}^{n} A_{li}(\chi, t)\dot{\chi}_i = c_l(\chi, t). \quad (11)$$

Equation (10) and its corresponding matrix form can be treated as a position constraint, while Equation (11) can be treated as a velocity constraint. Both A_{li} and c_l are first-order differentiable continuous functions. The (11) can be reorganized as follows:

$$A(\chi, t)\dot{\chi} = c(\chi, t), \quad (12)$$

where $A = [A_{li}]_{m\times n}$ and $c = [c_1, c_2, \ldots, c_m]^T$.

By differentiating (11) with respect to time t, we get

$$\sum_{i=1}^{n} A_{li}(\chi, t)\ddot{\chi}_i = -\sum_{i=1}^{n}\left(\frac{d}{dt}A_{li}(\chi, t)\right)\dot{\chi}_i + \frac{d}{dt}c_l(\chi, t) \quad (13)$$

Rewriting the above expression in matrix form, the constraint in the second-order form is then obtained:

$$A(\chi, t)\ddot{\chi} = b(\chi, \dot{\chi}, t). \quad (14)$$

Remark 1: It has been illustrated in many works (see References [23]–[26]) that the second-order constraint can be used directly in different control issues such as trajectory tracking, stability analysis and optimality. Obviously, Equation (14) is an acceleration type of constraint and it is linear with the acceleration. The information that satisfies the zero-order and first-order initial conditions is still retained in the initial conditions of the second-order constraint (i.e., Equation (14)).

Assumption 2: The matrix $A(\chi, t)$ is of full rank for $(\chi, t) \in \mathbf{R}^n \times \mathbf{R}$. There exists at least one vector solution $\ddot{\chi}_0$ to Equation (14).

Remark 2: The Assumption 2 actually means that all constraints applied to the system should be reasonable and there is no conflict or contradiction between all constraints.

Now let

$$\tau_1(t) = \bar{M}^{\frac{1}{2}}(\chi)(A(\chi, t)\bar{M}^{\frac{1}{2}}(\chi))^{+}[b(\dot{\chi}, \chi, t) + A(\chi, t)\bar{M}^{-1}(\chi)(\bar{C}(\dot{\chi}, \chi)\dot{\chi} + \bar{G}(\chi))]. \quad (15)$$

Here the τ_1 denotes the first part of the control and it originates from the UKFE. For the given constraint (14), the system will meet the constraints if the control has the form of (15). That is, the τ_1 in (15) is the ideal case of the control. The superscript "+" here denotes the Moore-Penrose (M-P) generalized inverse matrix. For a matrix M, its M-P generalized inverse matrix M^+ defers to the following algorithm:

$$M^+MM^+ = M^+, \quad (16)$$
$$MM^+M = M, \quad (17)$$
$$M^+M = (M^+M)^T, \quad (18)$$
$$MM^+ = (MM^+)^T. \quad (19)$$

Assumption 3: Based on the Assumption 2, for a given positive definite matrix $\Omega \in \mathbf{R}^{m\times m}$, and let:

$$H(\chi, \delta, t) = \Omega A(\chi, t)P(\chi)D(\chi, \delta)\bar{M}(\chi)A(\chi, t)^T \times (A(\chi, t)A^T(\chi, t))^{-1}\Omega^{-1}. \quad (20)$$

There exists a possibly unknown constant $\rho_c > -1$ and for all $(\chi, t) \in \mathbf{R}^n \times \mathbf{R}$,

$$\frac{1}{2}\min_{\delta\in\Sigma}\lambda_{\min}(H(\chi, \delta, t) + H^T(\chi, \delta, t)) \ge \rho_c. \quad (21)$$

Then, let

$$\tau_2(t) = -k_c\bar{M}(\chi)A^T(\chi, t)(A(\chi, t)A^T(\chi, t))^{-1} \times \Omega^{-1}\Upsilon(\dot{\chi}, \chi, t), \quad (22)$$

where $\Upsilon(\dot{\chi}, \chi, t) = A(\chi, t)\dot{\chi} - c(\chi, t)$, thereby $\dot{\Upsilon}(\dot{\chi}, \chi, t) = A(\chi, t)\ddot{\chi} - b(\chi, \dot{\chi}, t)$. The $\Upsilon(\dot{\chi}, \chi, t)$ can represent the tracking error of the constraint. If there exists following error of constraint, this part of control is a negative feedback to drive the system to follow the constraint. Hence, the τ_2 can be treated as the second part of the control.

Assumption 4: (i) For any $(\dot{\chi}, \chi, t) \in \mathbf{R}^n \times \mathbf{R}^n \times \mathbf{R}$ and $\delta \in \Sigma$, there exists a known function $\Gamma(\alpha, \dot{\chi}, \chi, t) \in \mathbf{R}_+$ with an unknown k dimensional constant vector $\alpha \in (0, \infty)^k$ such that

$$(1 + \rho_c)^{-1}\max_{\delta\in\Sigma}[\Big\|\Omega A(\chi, t)\tilde{P}(\chi, \delta)(-C(\dot{\chi}, \chi, \delta)\dot{\chi} - G(\chi, \delta) + \tau_1(t) + \tau_2(t)) - \Omega A(\chi, t)P(\chi) \times (\tilde{C}(\dot{\chi}, \chi, \delta)\dot{\chi} + \tilde{G}(\chi, \delta))\Big\| \le \Gamma(\alpha, \dot{\chi}, \chi, t), \quad (23)$$

(ii) for any $(\alpha, \dot{\chi}, \chi, t)$, the function $\Gamma(\alpha, \dot{\chi}, \chi, t)$ can be decomposed into the product of α^T and a column vector function, that is to say, there exists a vector function $\tilde{\Gamma}(\dot{\chi}, \chi, t) \in \mathbf{R}_+^k$ such that:

$$\Gamma(\alpha, \dot{\chi}, \chi, t) = \alpha^T\tilde{\Gamma}(\dot{\chi}, \chi, t). \quad (24)$$

Now we propose the controller as follows:

$$\tau(t) = \tau_1(t) + \tau_2(t) + \tau_3(\tilde{\alpha}, t), \tag{25}$$

where

$$\begin{aligned}\tau_3(\tilde{\alpha}, t) = &-[\bar{M}(\chi)A^T(\chi, t)(A(\chi, t)A^T(\chi, t))^{-1}\Omega^{-1}] \\ &\times \mu(\tilde{\alpha}, \dot{\chi}, \chi, t)\sigma(\tilde{\alpha}, \dot{\chi}, \chi, t)\Gamma(\tilde{\alpha}, \dot{\chi}, \chi, t),\end{aligned} \tag{26}$$

and for a positive real number $\varepsilon \in \mathbf{R}_+$,

$$\sigma(\tilde{\alpha}, \dot{\chi}, \chi, t) = \Upsilon(\dot{\chi}, \chi, t)\Gamma(\tilde{\alpha}, \dot{\chi}, \chi, t), \tag{27}$$

$$\mu(\tilde{\alpha}, \dot{\chi}, \chi, t) = \begin{cases} \left\|\sigma^{-1}(\tilde{\alpha}, \dot{\chi}, \chi, t)\right\|, & if \ \ \|\sigma(\cdot)\| > \varepsilon, \\ \varepsilon^{-1}, & if \ \ \|\sigma(\cdot)\| \le \varepsilon. \end{cases} \tag{28}$$

Here $\sigma(\cdot)$ denotes $\sigma(\tilde{\alpha}, \dot{\chi}, \chi, t)$. The τ_3 term (treated as the third part of control) is designed to deal with the control fluctuation caused by system uncertainty. The vector $\tilde{\alpha}$ in τ_3 is designed to estimate the unknown vector α, and τ_3 changes with the change of $\tilde{\alpha}$ to compensate for the uncertainty.

The adaptive vector $\tilde{\alpha}$ follows the following law:

$$\dot{\tilde{\alpha}} = k_a\tilde{\Gamma}(\dot{\chi}, \chi, t)\,\|\Upsilon(\dot{\chi}, \chi, t)\| - k_b\tilde{\alpha}, \tag{29}$$

where $k_{a,b} \in \mathbf{R}_+$. For the adaptive law of (29), $\tilde{\alpha}_i(t_0) > 0$, where $\tilde{\alpha}_i(t_0)$ is the i-th element of vector $\tilde{\alpha}$ at time t_0. Since $\tilde{\alpha}_i(t_0)$ is a positive value, $\tilde{\alpha}_i(t) > 0$ for all $t > t_0$. The value of vector $\tilde{\alpha}$ will increase rapidly to restrain the further increase of the error when the following error of the system increases. The $\tilde{\alpha}$ will decrease when the position of the system is close to the ideal position.

Theorem 1: Let $\psi := [\Upsilon^T, (\tilde{\alpha} - \alpha)^T]^T \in \mathbf{R}^{n+k}$. Suppose the mechanical system (8) is subjected to the constraints (14), the controller has the following performance under the assumptions 1-4:

(i) Uniform boundedness: For any $r > 0$, there exists a finite positive real number $d(r)$, if $\|\psi(t_0)\| \le r$, then $\|\psi(t)\| \le d(r)$ for all $t \ge t_0$.

(ii) Uniform ultimate boundedness: For any $r > 0$ and $\bar{d} > \underline{d}$ ($\underline{d} > 0$), if $\|\psi(t_0)\| \le r$, then $\|\psi(t)\| \le \bar{d}$ when $t \ge t_0 + T(\bar{d}, r)$, where $T(\bar{d}, r) < \infty$.

In order to analyze the stability of the controller, a reasonable Lyapunov function is given as

$$V(\Upsilon, \tilde{\alpha}) = \Upsilon^T\Omega\Upsilon + {k_a}^{-1}(1 + \rho_c)(\tilde{\alpha} - \alpha)^T(\tilde{\alpha} - \alpha). \tag{30}$$

For the sake of simplicity, we have omitted the parameters in the function except for some ambiguous places. Taking the first order derivative of (30) with respect to t, we have

$$\dot{V} = 2\Upsilon^T\Omega\dot{\Upsilon} + 2{k_a}^{-1}(1 + \rho_c)(\tilde{\alpha} - \alpha)^T\dot{\tilde{\alpha}}. \tag{31}$$

Next, let's analyze the content on the right side of equation (31) term by term. By introducing (8) into the first term on the right side of (31), we can get

$$\begin{aligned}2\Upsilon^T\Omega\dot{\Upsilon} &= 2\Upsilon^T\Omega(A\ddot{\chi} - b) \\ &= 2\Upsilon^T\Omega\left\{A\left[M^{-1}(-C\dot{\chi} - G) \right.\right. \\ &\quad \left.\left. + M^{-1}(\tau_1 + \tau_2 + \tau_3)\right] - b\right\},\end{aligned} \tag{32}$$

where

$$M^{-1} = P + \tilde{P}, \quad -C\dot{\chi} - G = (-\bar{C}\dot{\chi} - \bar{G}) + (-\tilde{C}\dot{\chi} - \tilde{G}). \tag{33}$$

Based on equation(33),

$$\begin{aligned}&A[M^{-1}(-C\dot{\chi} - G) + M^{-1}(\tau_1 + \tau_2 + \tau_3)] - b \\ &= A[(P + \tilde{P})(-\bar{C}\dot{\chi} - \bar{G} - \tilde{C}\dot{\chi} - \tilde{G}) + (P + \tilde{P}) \\ &\quad \times (\tau_1 + \tau_2 + \tau_3)] - b \\ &= A[P(-\bar{C}\dot{\chi} - \bar{G}) + P(\tau_1 + \tau_2) + P(-\tilde{C}\dot{\chi} - \tilde{G}) \\ &\quad + \tilde{P}(-C\dot{\chi} - G + \tau_1 + \tau_2) + (P + \tilde{P})\tau_3] - b.\end{aligned} \tag{34}$$

Next, by (15), we have $A[P(-\bar{C}\dot{\chi} - \bar{G}) + P\tau_1] - b = 0$. From Assumption 4(i),

$$\begin{aligned}&2\Upsilon^T\Omega A[\tilde{P}(-C\dot{\chi} - G + \tau_1 + \tau_2) + P(-\tilde{C}\dot{\chi} - \tilde{G})] \\ &\le 2\,\|\Upsilon\|\left\|\Omega A[\tilde{P}(-C\dot{\chi} - G + \tau_1 + \tau_2) + P(-\tilde{C}\dot{\chi} - \tilde{G})]\right\| \\ &\le 2\,\|\Upsilon\|\,(1 + \rho_c)\Gamma(\alpha, \dot{\chi}, \chi, t).\end{aligned} \tag{35}$$

Based on (22),

$$\begin{aligned}2\Upsilon^T\Omega AP\tau_2 &= 2\Upsilon^T\Omega AP[-k_c\bar{M}A^T(AA^T)^{-1}\Omega^{-1}(A\dot{\chi} - c)] \\ &= 2\Upsilon^T(-k_c)(A\dot{\chi} - c) = -2k_c\|\Upsilon\|^2.\end{aligned} \tag{36}$$

According to (26),

$$\begin{aligned}&2\Upsilon^T\Omega A(P + \tilde{P})\tau_3 \\ &= 2\Upsilon^T\Omega AP\{-[\bar{M}A^T(AA^T)^{-1}\Omega^{-1}]\mu\sigma\Gamma(\tilde{\alpha}, \dot{\chi}, \chi, t)\} \\ &\quad + 2\Upsilon^T\Omega APD\{-[\bar{M}A^T(AA^T)^{-1}\Omega^{-1}] \\ &\quad \times \mu\sigma\Gamma(\tilde{\alpha}, \dot{\chi}, \chi, t)\}.\end{aligned} \tag{37}$$

By applying equation (27), we have

$$\begin{aligned}&2\Upsilon^T\Omega AP\{-[\bar{M}A^T(AA^T)^{-1}\Omega^{-1}]\mu\sigma\Gamma(\tilde{\alpha}, \dot{\chi}, \chi, t)\} \\ &= -2(\Upsilon\Gamma(\tilde{\alpha}, \dot{\chi}, \chi, t))^T\mu\sigma \\ &= -2\sigma^T\mu\sigma = -2\mu\|\sigma\|^2.\end{aligned} \tag{38}$$

According to the Rayleigh principle [27], we have

$$\begin{aligned}&2\Upsilon^T\Omega APD\{-[\bar{M}A^T(AA^T)^{-1}\Omega^{-1}]\mu\sigma\Gamma(\tilde{\alpha}, \dot{\chi}, \chi, t)\} \\ &= -2\mu\sigma^T 1/2\{[\Omega APD\bar{M}A^T(AA^T)^{-1}\Omega^{-1}] \\ &\quad + [\Omega APD\bar{M}A^T(AA^T)^{-1}\Omega^{-1}]^T\}\sigma \\ &\le -2\mu\frac{1}{2}\lambda_m(H + H^T)\|\sigma\|^2 \le -2\mu\rho_c\|\sigma\|^2.\end{aligned} \tag{39}$$

Based on (37) and (38), we have

$$2\Upsilon^T\Omega A(P + \tilde{P})\tau_3 \le -2\mu(1 + \rho_c)\|\sigma\|^2. \tag{40}$$

Recall that if $\|\sigma\| > \varepsilon$,$-2\mu(1 + \rho_c)\|\sigma\|^2 = -2\frac{1}{\|\sigma\|}(1 + \rho_c)\|\sigma\|^2 = -2(1+\rho_c)\|\sigma\|$. If $\|\sigma\| \le \varepsilon$, $-2\mu(1+\rho_c)\|\sigma\|^2 = -2\frac{\|\sigma\|^2}{\varepsilon}(1 + \rho_c)$. By combining (35), (36), and (40), for all $\|\sigma\| > \varepsilon$,

$$\begin{aligned}2\Upsilon^T\Omega\dot{\Upsilon} \le &-2k_c\|\Upsilon\|^2 - 2(1 + \rho_c)\|\sigma\| \\ &+ 2\,\|\Upsilon\|\,(1 + \rho_e)\Gamma(\alpha, \dot{\chi}, \chi, t),\end{aligned} \tag{41}$$

for all $\|\sigma\| \le \varepsilon$,

$2\Upsilon^T\Omega\dot{\Upsilon}$

$$\leq -2k_c\|\Upsilon\|^2 - 2\frac{\|\sigma\|^2}{\varepsilon}(1+\rho_c) + 2\|\Upsilon\|(1+\rho_e) \times \Gamma(\alpha, \dot{\chi}, \chi, t)$$
$$= -2k_c\|\Upsilon\|^2 + (1+\rho_c)[-2\frac{\|\sigma\|^2}{\varepsilon} + 2\|\Upsilon\|\Gamma(\tilde{\alpha}, \dot{\chi}, \chi, t)] + (1+\rho_c)[-2\|\Upsilon\|\Gamma(\tilde{\alpha}, \dot{\chi}, \chi, t) + 2\|\Upsilon\|\Gamma(\alpha, \dot{\chi}, \chi, t)]. \quad (42)$$

For the part $-2\frac{\|\sigma\|^2}{\varepsilon} + 2\|\Upsilon\|\Gamma(\tilde{\alpha}, \dot{\chi}, \chi, t)$, its maximum value is $\frac{\varepsilon}{2}(1+\rho_c)$. Then, we have

$$2\Upsilon^T\Omega\dot{\Upsilon} \leq -2k_c\|\Upsilon\|^2 + \frac{\varepsilon}{2}(1+\rho_c) + (1+\rho_c) \times [-2\|\Upsilon\|\Gamma(\tilde{\alpha}, \dot{\chi}, \chi, t) + 2\|\Upsilon\|\Gamma(\alpha, \dot{\chi}, \chi, t)]. \quad (43)$$

According to Assumption 4(ii),

$$-2\|\Upsilon\|\Gamma(\tilde{\alpha}, \dot{\chi}, \chi, t) + 2\|\Upsilon\|\Gamma(\alpha, \dot{\chi}, \chi, t) = -2\|\Upsilon\|\tilde{\alpha}^T\tilde{\Gamma}(\dot{\chi}, \chi, t) + 2\|\Upsilon\|\alpha^T\tilde{\Gamma}(\dot{\chi}, \chi, t) = 2\|\Upsilon\|(\alpha - \tilde{\alpha})^T\tilde{\Gamma}(\dot{\chi}, \chi, t). \quad (44)$$

Then, for all $\|\sigma\|$,

$$2\Upsilon^T\Omega\dot{\Upsilon} \leq -2k_c\|\Upsilon\|^2 + \frac{\varepsilon}{2}(1+\rho_c) + 2\|\Upsilon\|(1+\rho_c)(\alpha - \tilde{\alpha})^T\tilde{\Gamma}(\dot{\chi}, \chi, t). \quad (45)$$

According to (29), the second term on the right side of (31) could be written as

$$2k_a{}^{-1}(\tilde{\alpha} - \alpha)^T\dot{\tilde{\alpha}}$$
$$= 2k_a{}^{-1}(\tilde{\alpha} - \alpha)^T(k_a\tilde{\Gamma}(\dot{\chi}, \chi, t)\|\Upsilon\| - k_b\tilde{\alpha})$$
$$= 2(\tilde{\alpha} - \alpha)^T\tilde{\Gamma}(\dot{\chi}, \chi, t)\|\Upsilon\| - 2k_a{}^{-1}k_b(\tilde{\alpha} - \alpha)^T(\tilde{\alpha} - \alpha + \alpha)$$
$$= 2(\tilde{\alpha} - \alpha)^T\tilde{\Gamma}(\dot{\chi}, \chi, t)\|\Upsilon\| - 2k_a{}^{-1}k_b(\tilde{\alpha} - \alpha)^T(\tilde{\alpha} - \alpha) - 2k_a{}^{-1}k_b(\tilde{\alpha} - \alpha)^T\alpha$$
$$\leq 2(\tilde{\alpha} - \alpha)^T\tilde{\Gamma}(\dot{\chi}, \chi, t)\|\Upsilon\| - 2k_a{}^{-1}k_b\|\tilde{\alpha} - \alpha\|^2 + 2k_a{}^{-1}k_b\|\tilde{\alpha} - \alpha\|\|\alpha\|. \quad (46)$$

Combining (45) and (46), we have

$$\dot{V} \leq -2k_c\|\Upsilon\|^2 + (1+\rho_c)\frac{\varepsilon}{2} - 2k_a{}^{-1}k_b(1+\rho_c)\|\tilde{\alpha} - \alpha\|^2 + 2k_a{}^{-1}k_b(1+\rho_c)\|\tilde{\alpha} - \alpha\|\|\alpha\|$$
$$\leq -\kappa_1\|\gamma\|^2 + \kappa_2\|\gamma\| + \kappa_3, \quad (47)$$

where $\|\gamma\|^2 = \|\Upsilon\|^2 + \|\tilde{\alpha} - \alpha\|^2$, $\|\tilde{\alpha} - \alpha\| \leq \|\gamma\|$, $\kappa_1 = \min\{2k_c, 2k_a{}^{-1}k_b(1+\rho_c)\}$, $\kappa_2 = 2k_a{}^{-1}k_b(1+\rho_c)\|\alpha\|$, $\kappa_3 = (1+\rho_c)\varepsilon/2$.

When $\|\gamma\| > (\kappa_2 + \sqrt{\kappa_2{}^2 + 4\kappa_1\kappa_3})/(2\kappa_1)$, the derivative of (47) is negative definite. According to References [28] and [29], the system is uniform boundedness with

$$d(r) = \begin{cases} \sqrt{\frac{\xi_2}{\xi_1}}R, & if\ r \leq R \\ \sqrt{\frac{\xi_2}{\xi_1}}r, & if\ r > R \end{cases}$$

$$R = \frac{1}{2\kappa_1}(\kappa_2 + \sqrt{\kappa_2{}^2 + 4\kappa_1\kappa_3}), \quad (48)$$

where $\xi_1 = \min\{\lambda_{min}(\Omega), (1+\rho_c)/k_a\}$, $\xi_2 = \max\{\lambda_{max}(\Omega), (1+\rho_c)/k_a\}$, and uniform ultimate boundedness with

$$\underline{d} = \sqrt{\frac{\xi_2}{\xi_1}}R,$$
$$T(\bar{d}, r) = \begin{cases} 0 & if\ r \leq \underline{d}\sqrt{\frac{\xi_2}{\xi_1}} \\ \frac{\xi_2 r^2 - (\xi_1{}^2/\xi_2)\bar{d}^2}{\kappa_1\bar{d}^2(\xi_1/\xi_2) - \kappa_2\bar{d}(\xi_1/\xi_2)^{1/2} - \kappa_3}. \end{cases} \quad (49)$$

IV. NUMERICAL SIMULATION

The total mass of mobile robot system may change during the motion process in some occasions, such as watering the plants, spraying pesticide, loading and unloading objects, etc. We choose $\bar{m} = 60$ kg, $\tilde{m} = 0.5\sin(t)$ kg, $I = 2$ kg $\cdot$ m^2, $l = 0.3$ m. At the same time, in order to satisfy Assumption 4, the function could be chosen as

$$\Gamma(\alpha, \dot{\chi}, \chi, t) = \alpha_1\|\dot{\chi}\|^2 + \alpha_2\|\dot{\chi}\| + \alpha_3 = \begin{bmatrix}\alpha_1 & \alpha_2 & \alpha_3\end{bmatrix}\begin{bmatrix}\|\dot{\chi}\|^2 \\ \|\dot{\chi}\| \\ 1\end{bmatrix} = \alpha^T\tilde{\Gamma}(\dot{\chi}, \chi, t), \quad (50)$$

where $\alpha = [\alpha_1, \alpha_2, \alpha_3]^T$ is an unknown constant vector. Under the premise of satisfying the Assumption 4, we can also choose the function $\Gamma(\alpha, \dot{\chi}, \chi, t)$ as follows

$$\alpha_1\|\dot{\chi}\|^2 + \alpha_2\|\dot{\chi}\| + \alpha_3 \leq \alpha(\|\dot{\chi}\|^2 + 2\|\dot{\chi}\| + 1) = \alpha(\|\dot{\chi}\| + 1)^2 = \alpha^T\tilde{\Gamma}(\dot{\chi}, \chi, t), \quad (51)$$

where $\alpha = \max\{\alpha_1, \alpha_2/2, \alpha_3\}$. Now, giving an expected trajectory (circle): $(X-1)^2 + (Y-0.5)^2 = 0.5^2$, the trajectory could also be written as:

$$\begin{cases} X = 0.5\sin t + 1 \\ Y = 0.5\cos t + 0.5. \end{cases} \quad (52)$$

By deriving (52), we can get the first and second order constraints in the form of (12) and (14) respectively:

$$A = \begin{bmatrix}1 & 0 & 0 \\ 0 & 1 & 0\end{bmatrix}, \quad c = \begin{bmatrix}0.5\cos t \\ -0.5\sin t\end{bmatrix},$$
$$b = \begin{bmatrix}-0.5\sin t \\ -0.5\cos t\end{bmatrix}.$$

We choose the parameters of adaptive robust control as: $\Omega = 1.4 \times I_{2\times 2}$, $k_c = 8$, $\varepsilon = 0.001$, $k_a = 2$, $k_b = 0.1$, and the initial condition:

$$\begin{cases} \chi_0 = (1.05, 0.95, \pi/6), \\ \dot{\chi}_0 = (0.1, 0.06, -0.02), \\ \tilde{\alpha}(0) = 0.15. \end{cases}$$

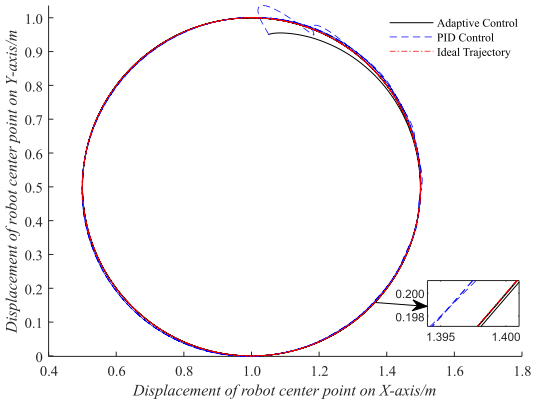

FIGURE 2. Trajectory diagram of the robot center point.

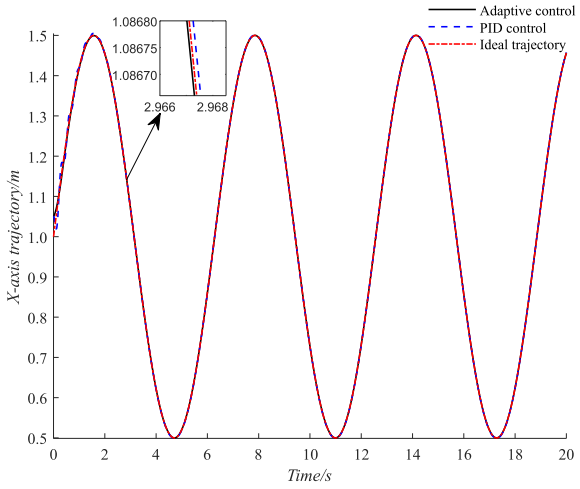

FIGURE 3. X-axis trajectory of center point.

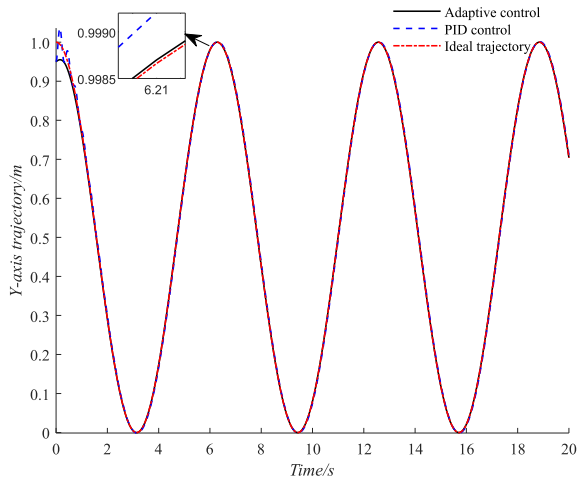

FIGURE 4. Y-axis trajectory of center point.

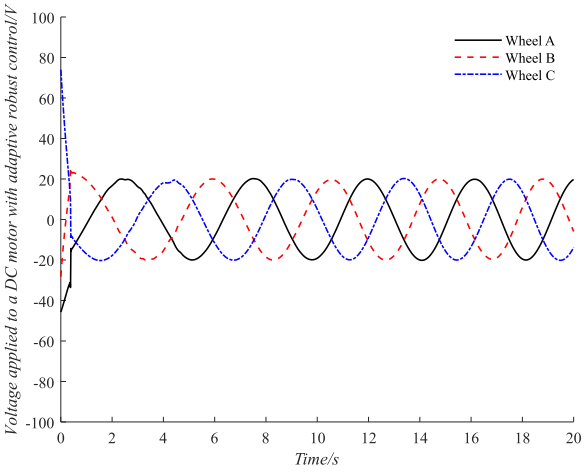

FIGURE 5. Control input.

It is noted that χ_0 is not strictly on the ideal trajectory, and we artificially give a deviation of the initial condition to test the effectiveness of the proposed method.

TABLE 2. Comparison of control performance of two methods.

Performance parameter	Adaptive robust control	PID control
$\bar{e}_x(m)$	4.6946×10^{-4}	0.0016
$\bar{e}_y(m)$	0.0013	0.0017
$e_{\max}(m)$	1.3513×10^{-4}	0.0015
$\bar{U}_A(V)$	12.9789	15.3474
$\bar{U}_B(V)$	12.7646	14.3483
$\bar{U}_C(V)$	13.5628	17.0365

Fig.2 shows the trajectories of the robot under the same condition using adaptive robust control and Proportion-Integration-Differentiation (PID) control, respectively. Comparing with the traditional PID control method, the trajectory of adaptive robust control basically coincides with the ideal trajectory and the error is much smaller than that under PID control. Table 2 shows the performance comparison of the two control methods when tracking the given circular trajectory. The parameters $\bar{e}_{x,y}$ in Table 2 are defined as $\bar{e}_{x,y} = \left(\int_0^T \left\|e_{x,y}(t)\right\|^2 dt/T\right)^{1/2}$, wherein T is the total time. The $\bar{e}_{x,y}$ denotes that the average value of the error between the actual position of the robot center point and the ideal position on each axis by neglecting the sign of the error. The $e_{\max} = \max\{e(t)\}, (t \geq t_s)$, which represent that the maximum error between the center point of the robot and the ideal position after reaching the stable state, wherein t_s is the time when the system error is stable. The $\bar{U}_{A,B,C} = (\int_0^T \left\|U_{A,B,C}\right\|^2 dt/T)^{1/2}$ which can represent the average control inputs of three drive motors by neglecting the sign of the input value.

From the data in Table 2, it can be concluded that the average tracking error, as well as the steady-state error under adaptive robust control are much more smaller than those under PID control when tracking the same trajectory. At the same time, the cost of control is reduced. Fig. 3 and Fig. 4 are obtained by decomposing the trajectory of the center point of the robot into X and Y axes, respectively. The partial enlarged drawing clearly shows that the trajectory of adaptive robust control is closer to the ideal trajectory. Fig. 5 shows the control input of each wheel. It can be seen from the

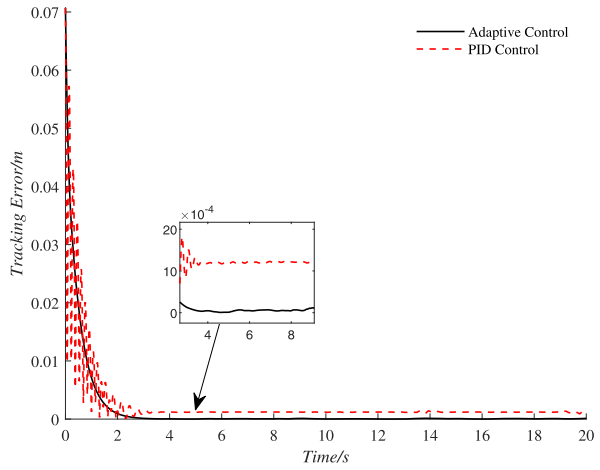

FIGURE 6. Error comparison.

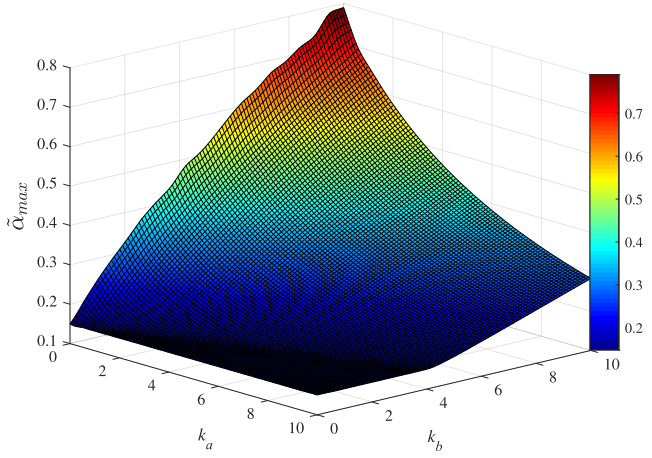

FIGURE 8. Effects of k_a and k_b on $\tilde{\alpha}_{max}$.

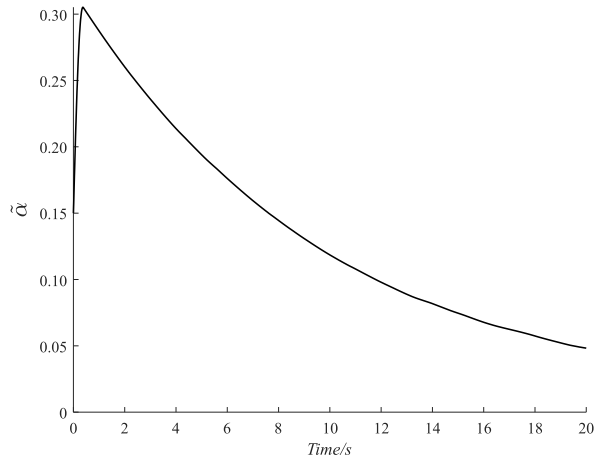

FIGURE 7. The change of adaptive parameters with time t.

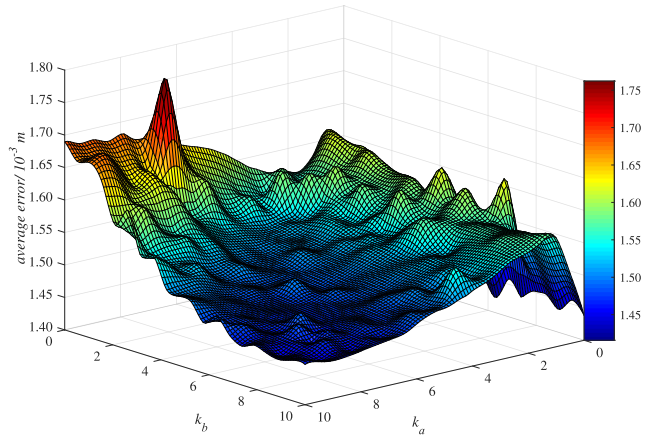

FIGURE 9. Effects of k_a and k_b on $\bar{e}$.

figure that the control input is relatively higher at the very beginning to reduce the error (recall that the initial position is far away from the ideal trajectory), and then decrease rapidly since the trajectory constraint is met quickly. The control input becomes stable after the following error goes into a stable area. Fig. 6 is the tracking error comparison diagram between adaptive robust control and PID control. After applying the proposed control τ, the tracking error is reduced to a small area near zero at about 2 seconds, and it has always been stabilized in that area over time. The tracking error of PID control fluctuates greatly before stabilization, and the maximum error of the PID control is 11 times more than that of the adaptive robust control after it stabilizes. Fig. 6 shows the outstanding performance of the adaptive robust control, that is, the error curve is smoother and converges to a neighborhood of 0. Fig. 7 shows the change of adaptive parameter $\tilde{\alpha}$ with time t. In the beginning, the value of $\tilde{\alpha}$ increases rapidly in order to suppress the deviation caused by the initial conditions. Comparing with Fig. 6, the $\tilde{\alpha}$ gradually decreases along with the reduction of the following error at $t = 2s$.

In addition, Fig. 8 and Fig. 9 show the effects of the design parameters k_a and k_b of the adaptive law on the maximum value of $\tilde{\alpha}$ and the average tracking error. It can be concluded that with the increase of k_b and the decrease of k_a, the maximum value of $\tilde{\alpha}$ in the control process increases and the average error will decrease at the same time. When the values of k_a and k_b are similar, the average error in the control process is the minimum, while the pair of larger k_a and the smaller k_b will increase the average error. This result provides us a reference to select the appropriate design parameters.

The trajectory of the above example is smooth. How about the control performance if the trajectory contains inflection point? Now, let's choose the expected trajectory of robot to be square which is expressed as:

$$\begin{cases} X = sign(\cos t)\cos^2 t \\ Y = sign(\sin t)\sin^2 t, \end{cases} \tag{53}$$

where *sign* stands for symbolic function. The trajectory constraints can be transformed into the forms of (12) and (14),

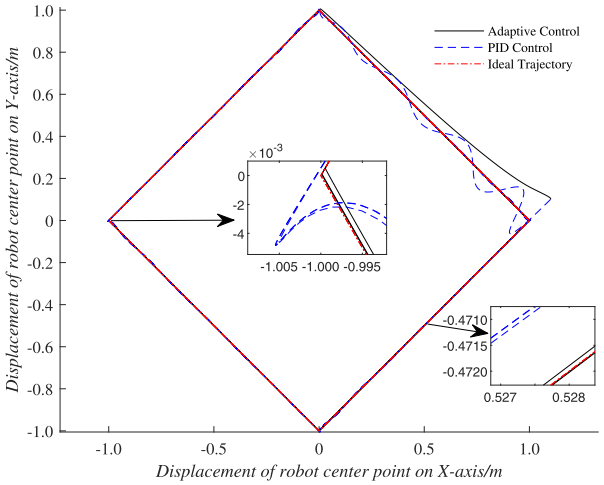

FIGURE 10. Square trajectory tracking results.

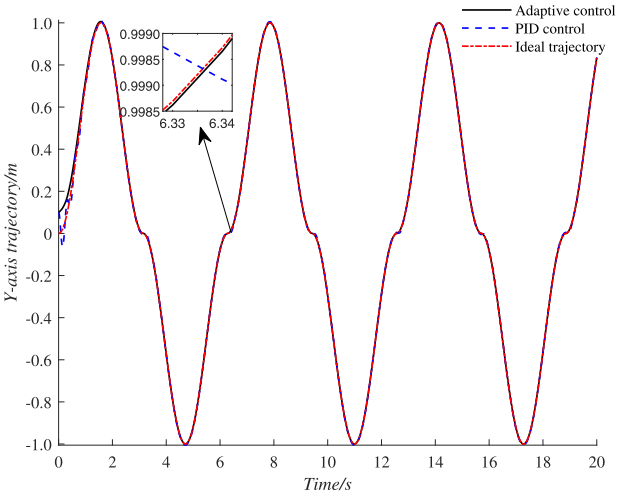

FIGURE 12. Y-axis trajectory of center point.

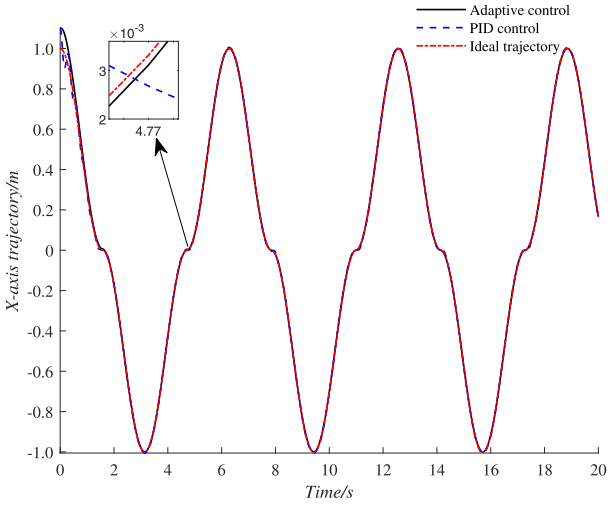

FIGURE 11. X-axis trajectory of center point.

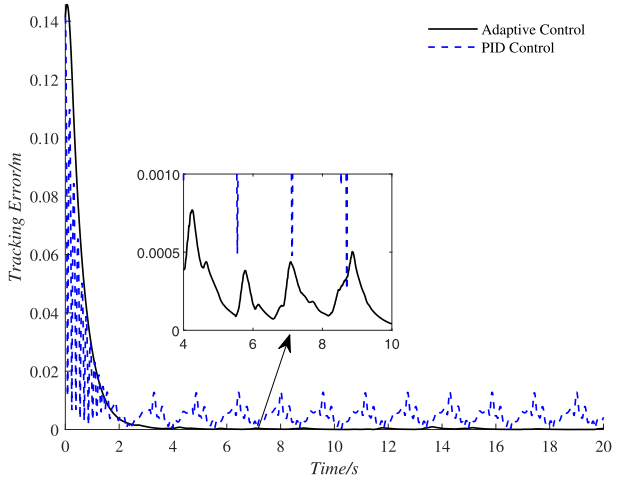

FIGURE 13. Y-axis trajectory of center point.

where

$$A = \begin{bmatrix} 1 & 0 & 0 \\ 0 & 1 & 0 \end{bmatrix}, \quad c = \begin{bmatrix} -2sign(\cos t)\sin t \cos t \\ 2sign(\sin t)\sin t \cos t \end{bmatrix},$$
$$b = \begin{bmatrix} -2sign(\cos t)(\cos^2 t - \sin^2 t) \\ 2sign(\sin t)(\cos^2 t - \sin^2 t) \end{bmatrix}.$$

Follow the same steps as the previous example, the initial condition is set as

$$\begin{cases} \chi_0 = (1.1, 0.1, \pi/6), \\ \dot{\chi}_0 = (0.1, 0.1, -0.02), \\ \tilde{\alpha}_0 = (0.15). \end{cases} \tag{54}$$

The parameters of controller and the uncertainty of the system are the same as the previous example. Fig. 10 shows the trajectory under the two control methods. It can be seen that the trajectory has an obvious overshoot at the corner of square when using PID control, while the adaptive robust control is smoother and the error is smaller in linear tracking. Fig. 11 and Fig. 12 show the comparison between the trajectory tracked by the two control methods and the ideal trajectory of the center point on each axis when tracking the square trajectory. Fig. 13 shows the total tracking error of the two control methods. We can also see that the error of PID control fluctuates greatly at the beginning. The error will increase when it meets the square inflection point, while the error of adaptive robust control is stable near zero after $t = 2s$.

The results of Fig. 2 to Fig. 13 verify the effectiveness of the proposed control method. The trajectory tracking control of omnidirectional mobile robot system can be realized even there exists uncertainties. Moreover, no matter whether the tracking curve is smooth or not, the adaptive robust control can always achieve better tracking performances.

V. CONCLUSION

An adaptive robust controller based on UKFE is designed and applied to the trajectory tracking of an omnidirectional wheeled mobile robot. The control method considers the uncertainty in the robot system, e.g., the mass in the system is not deterministic. Most of the conventional trajectory

tracking control methods take the tracking error as the state variable to meet the corresponding requirements, and are lack of robustness for the system with uncertainties. The control method in this paper abstracts the expected trajectory as virtual constraints so that the trajectory tracking problem is converted to servo constraint following control problem. The required constraint force can be obtained in the analytical form via UKFE. This method is similar to mimic the way of how nature meets constraints. An adaptive robust part is designed to suppress the impact of uncertainty. No more information is needed except for the existence of uncertainty bound. Both the effectiveness and reliability of the method are verified by theoretical proof and simulation experiment. Moreover, it can satisfy the uniform boundedness and uniform ultimate boundedness of the system in the control process. Compared with traditional PID control, it is derived from a quite different way and has better tracking performance, lower control costs.

REFERENCES

[1] J. H. Lee, C. Lin, H. Lim, and J. M. Lee, "Sliding mode control for trajectory tracking of mobile robot in the RFID sensor space," *Int. J. Control, Autom. Syst.*, vol. 7, no. 3, pp. 429–435, Jun. 2009.
[2] Y. Yi, F. Mengyin, S. Changsheng, W. Meiling, and Z. Cheng, "Control law design of mobile robot trajectory tracking and development of simulation platform," in *Proc. Chin. Control Conf.*, Hunan, Chine, Jul. 2006, pp. 198–202, doi: 10.1109/CHICC.2006.4347355.
[3] T. Kalmár-Nagy, R. D'Andrea, and P. Ganguly, "Near-optimal dynamic trajectory generation and control of an omnidirectional vehicle," *Robot. Auton. Syst.*, vol. 46, no. 1, pp. 47–64, Jan. 2004.
[4] F. E. Udwadia and R. E. Kalaba, *Analytical Dynamics: A New Approach*. Cambridge, U.K.: Cambridge Univ. Press, 1996.
[5] F. E. Udwadia and R. E. Kalaba, "A new perspective on constrained motion," *Proc. Roy. Soc. London A, Math. Phys. Sci.*, vol. 439, no. 1906, pp. 407–410, Nov. 1992.
[6] F. E. Udwadia and R. E. Kalaba, "Explicit equations of motion for mechanical systems with nonideal constraints," *J. Appl. Mech.*, vol. 68, no. 3, pp. 462–467, May 2001.
[7] R. Yu, H. Zhao, S. Zhen, K. Huang, X. Chen, H. Sun, and K. Zhang, "A novel trajectory tracking control of AGV based on Udwadia-Kalaba approach," *IEEE/CAA J. Autom. Sinica*, early access, Nov. 9, 2017, doi: 10.1109/JAS.2016.7510139.
[8] H. Sun, Y. H. Chen, K. Huang, and M. Qiu, "Controlling the differential mobile robot with system uncertainty: Constraint-following and the adaptive robust method," *J. Vib. Control*, vol. 25, pp. 1–12, Jan. 2019.
[9] L. Xin, Q. Wang, J. She, and Y. Li, "Robust adaptive tracking control of wheeled mobile robot," *Robot. Auton. Syst.*, vol. 78, pp. 36–48, Apr. 2016.
[10] M. Cui, W. Liu, H. Liu, H. Jiang, and Z. Wang, "Extended state observer-based adaptive sliding mode control of differential-driving mobile robot with uncertainties," *Nonlinear Dyn.*, vol. 83, nos. 1–2, pp. 667–683, Jan. 2016.
[11] F. N. Martins, W. C. Celeste, R. Carelli, M. Sarcinelli-Filho, and T. F. Bastos-Filho, "An adaptive dynamic controller for autonomous mobile robot trajectory tracking," *Control Eng. Pract.*, vol. 16, no. 11, pp. 1354–1363, Nov. 2008.
[12] W. He, Y. Chen, and Z. Yin, "Adaptive neural network control of an uncertain robot with full-state constraints," *IEEE Trans. Cybern.*, vol. 46, no. 3, pp. 620–629, Mar. 2016.
[13] S. X. Yang, A. Zhu, G. Yuan, and M. Q. Meng, "A bioinspired neurodynamics-based approach to tracking control of mobile robots," *IEEE Trans. Ind. Electron.*, vol. 59, no. 8, pp. 3211–3220, Aug. 2012.
[14] X. Liu, S. Zhen, H. Zhao, H. Sun, and Y.-H. Chen, "Fuzzy-set theory based optimal robust design for position tracking control of permanent magnet linear motor," *IEEE Access*, vol. 7, pp. 153829–153841, 2019.
[15] M. Pan, H. Wang, B. Gu, X. Qiu, and Y.-H. Chen, "A hierarchical robust control design with non-parallel distributed compensator and application to aircraft engines," *IEEE Access*, vol. 7, pp. 144813–144825, 2019.
[16] H. Sun, R. Yu, Y.-H. Chen, and H. Zhao, "Optimal design of robust control for fuzzy mechanical systems: Performance-based leakage and confidence-index measure," *IEEE Trans. Fuzzy Syst.*, vol. 27, no. 7, pp. 1441–1455, Jul. 2019.
[17] Q. Sun, G. Yang, X. Wang, and Y.-H. Chen, "Adaptive-adaptive robust (A2R) control for uncertain mechanical systems: Rendering β-ultimate boundedness," *IEEE Access*, vol. 7, pp. 176552–176564, 2019.
[18] J. Xu, F. Zeng, Y.-H. Chen, and H. Guo, "Robust constraint following stabilization for mechanical manipulators containing uncertainty: An adaptive φ approach," *IEEE Access*, vol. 6, pp. 58728–58736, 2018.
[19] H. Sun, R. Yu, Y.-H. Chen, and H. Zhao, "Optimal design of robust control for fuzzy mechanical systems: Performance-based leakage and confidence-index measure," *IEEE Trans. Fuzzy Syst.*, vol. 27, no. 7, pp. 1441–1455, Jul. 2019.
[20] R. Zhao, Y.-H. Chen, S. Jiao, X. Ma, and L. Wu, "Adaptive robust constraint-following control for mechanical systems with leakage and dead-zone," in *Proc. IEEE 56th Annu. Conf. Decis. Control (CDC)*, Melbourne, VIC, Australia, Dec. 2017, pp. 3308–3315, doi: 10.1109/CDC.2017.8264145.
[21] X. Wang, H. Zhao, Q. Sun, and Y.-H. Chen, "Regulating constraint obedience for fuzzy mechanical systems based on β-measure and a general Lyapunov function," *IEEE Trans. Fuzzy Syst.*, vol. 25, no. 6, pp. 1729–1740, Dec. 2017.
[22] Y.-H. Chen and X. Zhang, "Adaptive robust approximate constraint-following control for mechanical systems," *J. Franklin Inst.*, vol. 347, no. 1, pp. 69–86, Feb. 2010.
[23] Y.-H. Chen, "Constraint-following servo control design for mechanical systems," *J. Vib. Control*, vol. 15, no. 3, pp. 369–389, Jan. 2009.
[24] H. Yin, J. Huang, and Y.-H. Chen, "Possibility-based robust control for fuzzy mechanical systems," *IEEE Trans. Fuzzy Syst.*, early access, Oct. 7, 2020, doi: 10.1109/TFUZZ.2020.3028940.
[25] X. Zhao, Y.-H. Chen, F. Dong, and H. Zhao, "Controlling uncertain swarm mechanical systems: A β-measure-based approach," *IEEE Trans. Fuzzy Syst.*, vol. 27, no. 6, pp. 1272–1285, Jun. 2019.
[26] X. Chen, S. Zhen, H. Sun, and H. Zhao, "Adaptive robust constraint-following control for lower limbs rehabilitation robot," in *Proc. IEEE Int. Conf. Mechatronics, Robot. Automat. (ICMRA)*, Hefei, China, May 2018, pp. 150–156, doi: 10.1109/ICMRA.2018.8490575.
[27] N. Boyd and J. W. Daniel, *Applied Linear Algebra*, 3rd ed. Upper Saddle River, NJ, USA: Prentice-Hall, 1988.
[28] H. Khalil, *Nonlinear Systems*, 3rd ed. Upper Saddle River, NJ, USA: Prentice-Hall, 2002.
[29] Y. H. Chen, "On the deterministic performance of uncertain dynamical systems," *Int. J. Control*, vol. 43, no. 5, pp. 1557–1579, May 1986.

FANGFANG DONG received the Ph.D. degree in mechanical engineering from the Hefei University of Technology, Hefei, China, in 2016.

From September 2014 to August 2015, he was a Visiting Ph.D. Student with the George W. Woodruff School of Mechanical Engineering, Georgia Institute of Technology, Atlanta, GA, USA. His research interests include fuzzy dynamical systems, multibody system modeling, mechanical system control, and robotics control.

DONG JIN received the bachelor's degree in engineering from the Anhui University of Architecture, in 2019. He is currently pursuing the master's degree in machinery manufacturing and automation with the Hefei University of Technology.

His main research interests include industrial robot, automatic control, and so on.

XIAOMIN ZHAO received the Ph.D. degree in mechanical engineering from the Hefei University of Technology, Hefei, China, in 2017.

From August 2013 to August 2015, she was a Visiting Ph.D. Student the George W. Woodruff School of Mechanical Engineering, Georgia Institute of Technology, Atlanta, GA, USA. Her research interests include fuzzy dynamical systems, mechanical system control, swarm intelligence, and vehicle active safety control.

JIANG HAN received the Ph.D. degree in engineering from the Hefei University of Technology.

He visited the Institute of Machine Tool Control and Production System (ISW), Stuttgart University, Germany, in 2005. He worked as a Visiting Scholar with the Department of Machinery (s.m.wu Manufacturing Research Center), University of Michigan, in 2010. He is currently a Professor and a Ph.D. Supervisor with the School of Mechanical Engineering, Hefei University of Technology. His main research interests include intelligent manufacturing and intelligent equipment, digital and networked manufacturing technology and systems, mechatronics technology and products, and so on.